Numerical and Experimental Study of Evaporative Heat Transfer from a Radial Micro-Channel Evaporator for an External Combustion Micro Heat Engine

HoKi Lee, Cecilia D. Richards, Robert F. Richards
School of Mechanical and Materials Engineering, Washington State University, Pullman, USA

Abstract: The present work focuses on the design of a micro-evaporator for a vapor-cycle external combustion micro engine. The micro-evaporator consists of a thin membrane with open, rectangular channels that run from the center of the membrane to its edges. Working fluid is pumped by capillary forces from a reservoir at the edge of the membrane to the center of the membrane, where it is evaporated. Results from both an experimental and a numerical study of the evaporative heat transfer from the micro-channels are presented. The experimental results are shown to validate the numerical model. The performance of the micro-channel evaporator is shown to be dominated by conduction across the thin membrane.

Key words: Micro Evaporator, Dynamic Micro Heat Engine

1. INTRODUCTION

While several groups have worked on internal combustion dynamic micro heat engines, fewer have reported progress on external combustion dynamic micro heat engines. These types of engines require heat exchangers to transfer heat from an external heat source to the working fluid. In particular, vapor-cycle external combustion micro-engines require either a micro–evaporator or micro-boiler transfer heat to evaporate liquid working fluid.

Unfortunately, there appears to be no work in the engineering literature describing the design of a micro–evaporator or boiler specifically for a micro heat engine. However, there has been a great deal of work published on evaporation and boiling from micro-channels. While most of this work has been motivated by microelectronic cooling, it can be applied to the present application of phase-change heat transfer in micro-engines.

For example, several groups have reported numerical and analytical models of evaporation from micro-channels. Naoki et al. presented an extended analytical theory of the capillary rise problem for a rectangular micro-channel in order to study the interface motion driven by capillary action in a micro-channel [3]. Nilson et al. derived numerical and analytical solutions for steady evaporating flow in open micro-channels having a rectangular cross section with uniform depth and decreasing width [4].

The present work builds upon previous experimental and numerical work [5, 6, 7, 8] to develop and extend a numerical model of evaporative heat transfer from square open-top micro-channels for the purpose of optimization of a micro-evaporator for vapor cycle micro heat engines. The micro-evaporator consists of a thin membrane with open-rectangular channels formed from straight rectangular-section walls that run from the center of the membrane to its edges. Working fluid is pumped from a reservoir at the edge of the membrane to the center of the membrane by capillary forces. Heat supplied at the center of the membrane evaporates the working fluid as it moves in. A numerical model of the micro-evaporator is developed. Experimental measurements on prototype micro-evaporators are used to validate the numerical model. Results from both the experimental and numerical work indicate that the performance of the micro-channel evaporator is shown to be dominated by conduction across the thin membrane.

2. THEORY

The numerical model calculates conduction heat transfer using axisymmetric finite difference time domain integration. A schematic of the numerical model is shown in Figure 1.

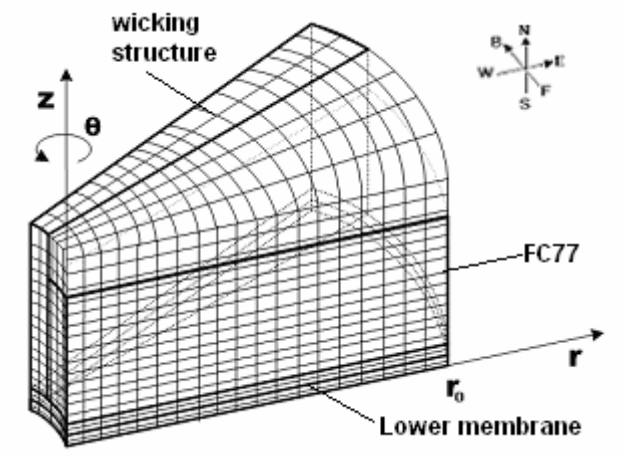

Figure 1. Schematic of axisymmetric numerical model

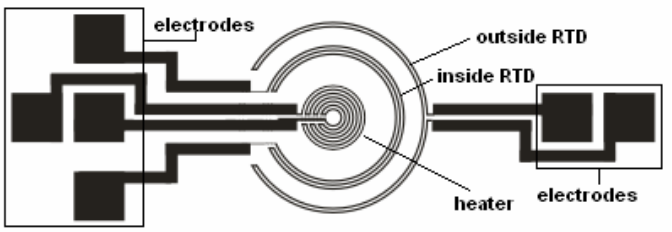

Figure 2. Experimental test die schematic.

The heat diffusion equation applied to heat conduction calculation in the membrane and liquid working fluid was:

$$\nabla^2 T = \frac{1}{\alpha}\frac{dT}{dt}$$

where T was temperature, α was thermal diffusivity, and t was time. Implicit finite difference time domain integration was used to solve the equation.

The mass transfer rate associated with evaporation from the liquid-vapor interface was determined from conservation of energy

$$q_v - q_l = 0$$

where

$$q_v = jAh_{fg} \text{ and } q_l = -\frac{k_l A}{L}(T_{sl} - T_l)$$

where h_{fg} was latent heat of working fluid, j was mass flux, k was thermal conductivity of membrane material, and L was thickness of liquid.

A force balance was used to determine capillary pumping rates for the liquid working fluid in the micro-channels.

3. EXPERIMENTAL

The experimental study was conducted using micro-channel evaporators fabricated on test die micro-machined from three-inch silicon wafers. Each test die consisted of a 5mm square, membrane on which a circular platinum resistance heater, two concentric annular platinum resistance thermometers (PRT's), and a radial wicking structure. Two types of membrane were used, 2 micron thick silicon membranes and 300 nanometer thick silicon nitride membranes. A schematic view of the test die is shown in Figure 2.

The radial micro-channels were fabricated by spinning on 40 microns of SU-8. Photolithography was used to define micro channels from 5 to 80 microns wide, bounded by 5 to 80 microns wide SU-8 walls. A thin-film resistance heater was fabricated at the center of membrane and the radial channels. Two annular platinum resistance heaters were fabricated at radii of 1.7 millimeters and 2.4 millimeters.

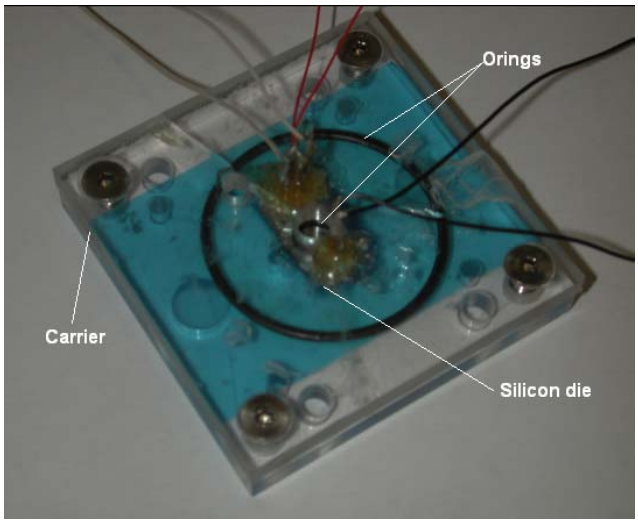

Figure 3. Photograph of microchannel evaporator die in its acrylic carrier.

The test die was mounted in an acrylic carrier with an outer reservoir of working fluid contained between two O-rings. The two o-rings controlled the fluid flowing from the reservoir. The working fluid was the fluorinert refrigerant, FC77, from Dupont. Capillary forces pumped fluid from the outer reservoir under the inner O-ring and into the microchannels covering the membrane. A photograph of the microchannel evaporator die mounted in the acrylic carrier is shown in Figure 3. The die and acrylic carrier were placed on a scale with a precision of ±0.5 mg.

An experiment was run by introducing Fluorinert FC77 working fluid at the outer circumference of the radial channels. Capillary forces wicked working fluid from the outer circumference into the center of the membrane. Electrical power was dissipated as heat in the central thin-film resistance heater. Sensible heat then conducted radially out through the membrane, and drove evaporation of liquid working fluid from the radial channels. An energy balance was then experimentally determined for the micro-channel evaporator test die. The major terms of interest in the energy balance were the: (1) Electrical power dissipated as heat in the central resistance heater, (2) Sensible heat conducted radially out through the membrane, and (3) Latent heat carried away from the membrane by evaporating working fluid.

In the present set of experiments, 30 *mW* to 60 *mW* of electrical power was dissipated in the thin-film heater at the center of the silicon membrane on the test die. The power dissipated as heat in the thin-film heater was determined by measuring the voltage drop across the platinum resistance heater and the voltage

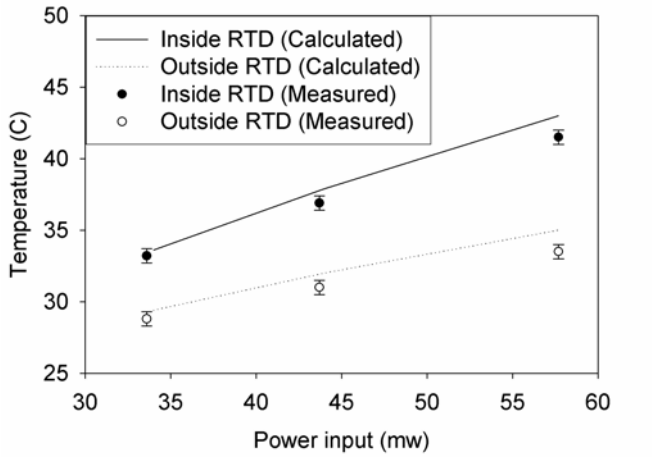

Figure 4. Temperature distribution in the Si microchannel evaporator versus power input.

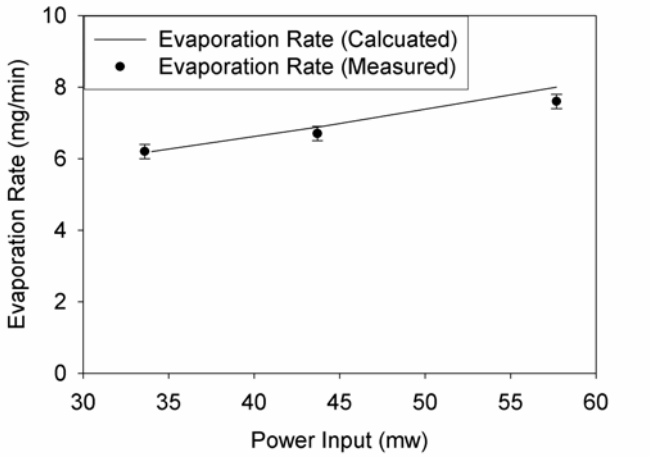

Figure 5. Evaporation rate from the Si microchannel evaporator versus power input.

drop across a power resistor in series with the heater. The uncertainty in power dissipated was 8%.

The sensible heat conducted radially out through the membrane was determined using the temperatures determined by the two concentric annular RTD's on each die. The two RTD's were each monitored using a Wheatstone bridge circuit. The RTD's and bridge circuits were calibrated by immersing the die into a temperature-controlled water bath. The uncertainty in temperature measurement of the RTD's was estimated to be within ±0.5ºC.

Conduction heat transfer out of the membrane was assumed to be radially symmetric so that the heat transfer rate, Q_s, was determined by:

$$Q_s = 2\pi kh \cdot \Delta T / \ln(r_o / r_i) \qquad (1)$$

where r_o and r_i were the radii of the outer and inner PRT's, k was the thermal conductivity of silicon, h was the thickness of the silicon membrane, and ΔT was the difference in PRT temperatures. The uncertainty in conductive heat transfer rate Q_s was ±3%.

The entire test die was situated on a sensitive balance in order to gravimetrically determine the mass transfer rate by evaporation. The latent heat transfer rate from the micro-channel evaporator was then taken to be:

$$Q_l = j\, h_{fg} \qquad (2)$$

where j was the rate of mass transfer by evaporation of working fluid from the micro-channels, and h_{fg} was the latent heat of evaporation of the working fluid. The uncertainty in mass transfer in latent heat transfer rate was ±5%.

3. DISCUSSION

The experimental results are shown to validate the numerical model as seen in Figs. 4 through 7. Figure 4 shows both experimental and predicted temperatures at the RTD locations for Si membranes for three input power settings. Figure 5 shows both measured and predicted evaporation rates Si membranes for the same three power settings. The model is seen to compare well with the experimental measurements. Figure 6 shows both experimental and predicted temperatures at the RTD locations for SiNx membranes for two power settings. Figure 7 shows both measured and predicted evaporation rates SiNx membranes for the same two power settings. Again the model compares well with the experiments.

Tables 1 and 2 give the energy balances for both Si and SiNx membrane microchannel evaporators. The fraction of power conducted out of the membrane is seen to be substantially lower for the low-conductivity SiNx membranes. Likewise the fraction of power going into evaporating working fluid is much larger for the SiNx membranes. Reducing the conductivity of the membrane is seen to increase the efficiency of the microchannel evaporator from 18-26% to 82-86%.

4. CONCLUSION

The design of a micro-evaporator for a vapor-cycle external combustion dynamic micro heat engine has been presented. Results from both an experimental and a numerical study of the evaporative heat transfer from the open-top micro-channels have been shown. The experimental results are shown to validate the numerical model.

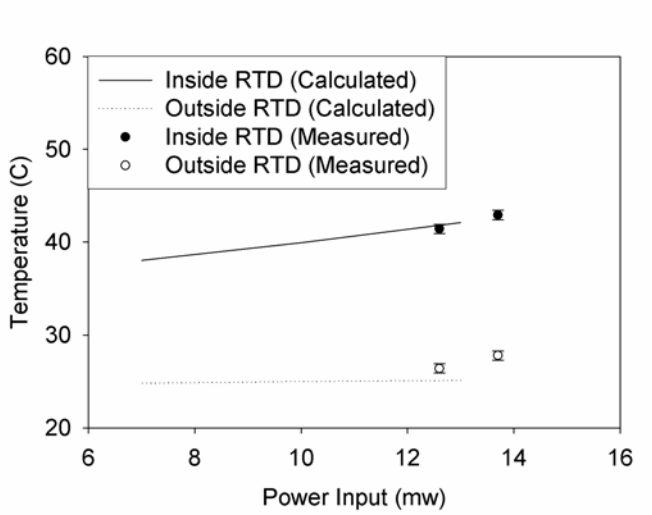

Figure 6. Temperature distribution in the SiNx microchannel evaporator versus power input.

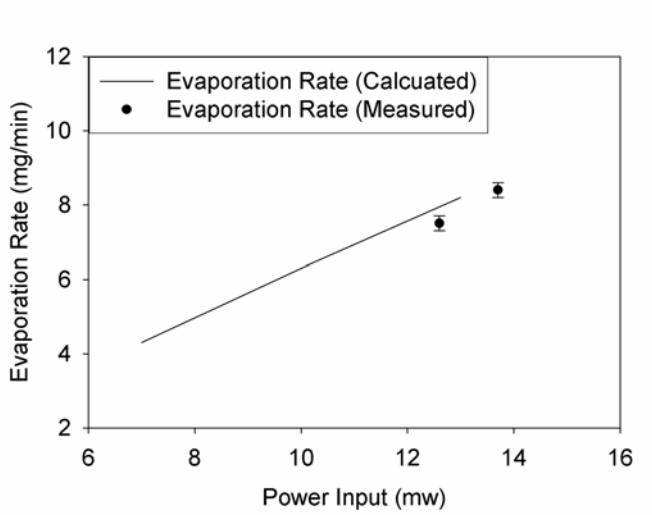

Figure 7. Evaporation rate from the SiNx microchannel evaporator versus power input.

SU8 Height (micron)	SU8 Wall Width (micron)	Channel Width (micron)	Power into Heater (mW)	Inside RTD Temp (°C)	Outside RTD Temp (°C)	Power across Membrane (mW)	Power into Evap (mW)	Evaporation Rate (mg/min)	Efficiency (%)
EXPERIMENTAL RESULTS									
40	5~80	5~80	34	33.2	28.8	24	8.6	6.2	26
			44	36.9	31.0	33	9.3	6.7	21
			58	41.5	33.5	45	10.6	7.6	18
NUMERICAL RESULTS									
40	5~80	5~80	34	33.6	29.4	25	8.6	6.2	25
			44	38.1	32.3	34	9.8	7.0	22
			57	42.8	34.7	46	11.0	8.0	19

Table 1. Energy balance for Si membrane microchannel evaporator.

SU8 Height (micron)	SU8 Wall Width (micron)	Channel Width (micron)	Power into Heater (mW)	Inside RTD Temp (°C)	Outside RTD Temp (°C)	Power across Membrane (mW)	Power into Evap (mW)	Evaporation Rate (mg/min)	Efficiency (%)
EXPERIMENTAL RESULTS									
40	5~80	5~80	14	42.9	27.8	1.2	12	8.4	86
			13	41.4	26.4	1.1	10	7.5	82
NUMERICAL RESULTS									
40	5~80	5~80	13	42.1	25.1	1.5	12	8.2	88
			10	39.9	25.0	1.3	9	6.3	87
			7	38.0	24.8	1.0	6	4.3	86

Table 2. Energy balance for SiNx membrane microchannel evaporator

The performance of the micro-channel evaporator is shown to be dominated by conduction across the thin membrane. Changing the membrane material from the high conductivity Si (two micron thick) to the low conductivity SiNx (three-hundred nanometer thick) is shown to significantly decreases heat losses from the evaporator by conduction through the membrane. The fraction of heat transferred to the evaporating working fluid is shown to go from roughly 30% to 90% of the heat added to the center of the micro-channel evaporator.

REFERENCES

[1] I. Tiselj, G. Hetsroni, B. Mavko, A. Mosyak, E. Pogrebnyak, Z. Segal, Effect of axial conduction on the heat transfer of micro-channels. International of Heat and Mass Transfer, 47 (2004) 2551-2565.

[2] C.B. Sobhan, S.V. Farimella, Micro-scale Thermophysical Engineering, 5, 293-311, 2001.

[3] I. Naoki, H, Kazuo, M. Ryutaro, Interface Motion of Capillary-driven Flow in Rectangular Microchannel. Journal of colloid and Interface Science 280 (2004) 155-164

[4] R.H. Nilson, S.W. Tchikanda, S.K. Griffinths, M.J. Martinez, Steady Evaporation Flow in Rectangular Micro-channels. Int. J. Heat and Mass Transfer, 49, 1603-1618, 2006

[5] S. A.Whalen, C.D. Richards, D.F. Bahr, R.F. Richards, Characterization and Modeling of Microcapillary Driven Liquid-Vapor Phase Change Membrane Actuator, Sensors and Actuators: A Physical, vol. 134, pp. 201-212, 2007.

[7] T.A. Quy, D. Carpenter, C.D. Richards, D.F. Bahr, R.F. Richards, Evaporative Heat Transfer from Ten-micron Micro-channels. ASME. IMECE, 2005

[8] HoKi Lee, T.A. Quy, C.D. Richards, D.F. Bahr, R.F. Richards, Experimental and Numerical Study of Evaporative Heat Transfer from Ten-micro Micro-channels. ASME. IMECE, 2006